AAS 23-229

LOW THRUST AUGMENTATION FOR BALLISTIC LUNAR TRANSFERS

Stephen T. Scheuerle[*], Kathleen C. Howell[†], and Diane C. Davis [‡]

Low-energy transfers offer propellant-efficient paths to the Moon. This investigation introduces techniques for constructing low-energy lunar transfers with a focus on the trade-offs between time-of-flight and propellant requirements, if any. A type of low-energy transfer, denoted a Ballistic Lunar Transfer (BLT), leverages the gravitational influence of the Sun to reduce the propellant cost upon arrival into orbits near the vicinity of the Moon. To model a spacecraft governed by the Earth-Moon-Sun system, the Bicircular Restricted Four-Body Problem (BCR4BP) is incorporated. To explore the range of possible transfer geometries, impulsive maneuvers and low-thrust transfer arcs are examined.

INTRODUCTION

Spacecraft trajectory design incorporates hardware constraints and desired mission outcomes to construct a feasible path through space. Mission trajectories that depart Earth toward the Moon often include limitations on time-of-flight and/or propellant. For vehicles with limited propellant capabilities or low-thrust propulsion, low-energy transfers are desirable. One type of low-energy transfer denoted a Ballistic Lunar Transfer (BLT), leverages solar perturbations over several months enroute to the Moon. Several missions in the past year employed BLTs to reach the Moon, including NASA's Cislunar Autonomous Positioning System Technology Operations and Navigation Experiment (CAPSTONE),[1] and the Korea Pathfinder Lunar Orbiter Mission (KPLO).[2] NASA's Lunar Flashlight and ispace's HAKUTO-1 missions are also actively leveraging BLTs to reach the lunar vicinity.[3,4] As the long time-of-flight required for a BLT may be undesirable for some mission scenarios, the introduction of low thrust or impulsive maneuvers offers trade-offs to reduce the overall transfer time. NASA's Lunar IceCube, a secondary payload on Artemis I, planned to leverage low thrust capabilities along with solar perturbations to enter orbit about the Moon.[5] The Khon-1 spacecraft is a secondary payload that intends to utilize low-energy transfers alongside low and high-thrust capabilities to reach lunar orbit.[6] As low-energy transfers often leverage the gravitational influence of the Sun, the combination of low thrust and solar perturbations offers unique mission options. Techniques employing low thrust supply varied options when designing missions to cislunar space. Intermediate strategies to reduce time-of-flight or accommodate for variations in epoch are applicable for certain mission profiles. Identifying favorable techniques for applying low thrust is necessary to the mission design process. The goal of this investigation is a general

[*]Ph.D. Student, School of Aeronautics and Astronautics, Purdue University, West Lafayette, IN 47907; sscheuer@purdue.edu

[†]Hsu Lo Distinguished Professor, School of Aeronautics and Astronautics, Purdue University, West Lafayette, IN 47907; howell@purdue.edu. Fellow AAS; Fellow AIAA

[‡]Aerospace Engineer, Johnson Space Center, Houston, TX, 77058; diane.c.davis@nasa.gov

framework to construct low-energy transfers to the Moon that incorporate low-thrust propulsion and highlight the appropriate trade-offs.

DYNAMICAL MODELS

Circular Restricted Three-body Problem

Periodic orbits in the CR3BP offer sample destinations in cislunar space for low-energy transfers. The CR3BP depicts the motion of a spacecraft (P_3) due to the gravitational influence of the Earth and Moon (P_1 and P_2). It is assumed that the mass of the spacecraft is negligible compared to the primary bodies, thus, the motion of the Earth and Moon is independent of the spacecraft location. The Earth and Moon are then assumed to follow circular orbits around their mutual barycenter (B_1). The mass of the Earth and Moon are M_1 and M_2, respectively. The CR3BP is nondimensionalized to simplify the equations of motion and aid in numerical implementation. The characteristic length and time are defined such that the non-dimensional distance between the two primary bodies is one, and the mean motion of the P_1-P_2 system is unity. Expressing the equations of motion in a coordinate frame that rotates with the primary bodies, the differential equations are time-independent.[7] The motion of the spacecraft (P_3) is described by three scalar nonlinear second-order differential equations, that are expressed as,

$$\ddot{x} = 2\dot{y} + \frac{\partial U}{\partial x} \qquad \text{(1a)} \qquad \ddot{y} = -2\dot{x} + \frac{\partial U}{\partial y} \qquad \text{(1b)} \qquad \ddot{z} = \frac{\partial U}{\partial z} \qquad \text{(1c)}$$

where x, y, z and $\dot{x}$, $\dot{y}$, $\dot{z}$ are the nondimensional position and velocity components of the spacecraft in the Earth-Moon rotating frame. The variables $\frac{\partial U}{\partial x}$, $\frac{\partial U}{\partial y}$, and $\frac{\partial U}{\partial z}$ are the partial derivatives of the pseudo-potential function U with respect to the position of P_3. The pseudo-potential function, U, is written as,

$$U = \frac{1}{2}\left(x^2 + y^2\right) + \frac{1-\mu}{r_{13}} + \frac{\mu}{r_{23}} \tag{2}$$

where the term μ is the mass parameter, defined $\mu = \frac{M_2}{M_1+M_2}$. The value r_{ij} is the scalar distance between body i and j. The CR3BP possesses a single integral of the motion. The integral of the motion is denoted the Jacobi Constant and remains fixed along a ballistic arc.[8] The Jacobi Constant value (JC) is written as,

$$JC = 2U - (\dot{x}^2 + \dot{y}^2 + \dot{z}^2) \tag{3}$$

The Jacobi Constant represents an 'energy-like' quantity, consisting of a pseudo-potential term and the norm of the rotating velocity components. As the square of the velocity terms are negative, an increase in the Jacobi Constant corresponds to a decrease in energy. For trajectories in the CR3BP, the Jacobi Constant adds insight into applying dynamical systems theory, including a basis for comparing two transfer energies and assessing bounded regions at a given energy level.

Bicircular Restricted Four-body Problem

The bicircular restricted four-body problem (BCR4BP) is the primary gravitational model incorporated in this analysis. The BCR4BP describes the motion of a massless particle (P_3) due to the gravitational field in the Earth-Moon-Sun system. The Earth and Moon are assumed to follow circular orbits about their mutual barycenter (B_1). The Sun and the Earth-Moon system are also assumed to follow circular orbits about the total system barycenter (B_2). The motion of the spacecraft with respect to the primary bodies (Earth, Moon, and Sun) may be expressed in an Earth-Moon or Sun-B_1 rotating frame. The Earth-Moon rotating quantities in the BCR4BP are defined with tildes, i.e., $(\widetilde{x}, \widetilde{y}, \widetilde{z})$. Terms expressed in the Sun-B_1 rotating frame are defined with underlined-quantities, i.e., $(\underline{x}, \underline{y}, \underline{z})$. The BCR4BP may be nondimensionalized in the respective rotating frames to aid in computational accuracy. For this analysis, the equations of motion are expressed in the Earth-Moon rotating frame. The model is nondimensionalized such that the distance between the Earth and Moon and the mean motion of the Earth-Moon system are set to a value of one. The equations of motion for P_3 in the BCR4BP are formulated relative to the Earth-Moon rotating frame, as

$$\ddot{\widetilde{x}} = 2\dot{\widetilde{y}} + \frac{\partial \Upsilon}{\partial \widetilde{x}} \quad \text{(4a)} \qquad \ddot{\widetilde{y}} = -2\dot{\widetilde{x}} + \frac{\partial \Upsilon}{\partial \widetilde{y}} \quad \text{(4b)} \qquad \ddot{\widetilde{z}} = \frac{\partial \Upsilon}{\partial \widetilde{z}} \quad \text{(4c)}$$

where Υ is the pseudo-potential function for the differential equations in the BCR4BP as represented in the Earth-Moon rotating frame. The pseudo-potential function is written as

$$\Upsilon = \frac{1}{2}(\widetilde{x}^2 + \widetilde{y}^2) + \frac{1-\mu}{r_{13}} + \frac{\mu}{r_{23}} + \frac{\widetilde{m}_S}{r_{43}} - \frac{\widetilde{m}_S}{r_S^2}(\widetilde{x}\cos(\theta_S) + \widetilde{y}\sin(\theta_S)) \tag{5}$$

where m_S is the non-dimensional mass of the Sun, i.e., $m_S = \frac{M_4}{M_1+M_2}$, r_S is the constant distance between the Sun and Earth-Moon barycenter, and r_{43} is the scalar distance from the Sun to the spacecraft. The Sun angle (θ_S) defines the location of the Sun in the Earth-Moon rotating frame and is illustrated in Figure 1(a). In the Sun-B_1 rotating coordinate frame, the Earth-Moon angle (θ_{EM}) orients the Earth and Moon line with respect to the Sun as apparent in Figure 1(b).

The instantaneous Jacobi Constant is employed to assess the variation in energy along a trans-

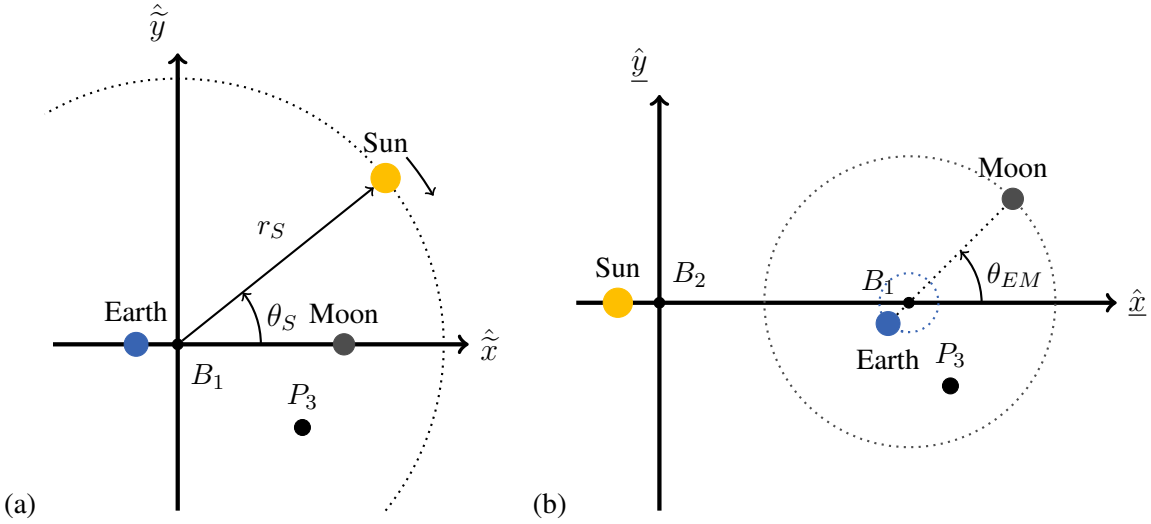

Figure 1. The Earth-Moon (a) and Sun-B_1 (b) rotating coordinate frames

fer. Recall that the Jacobi Constant value is an integral of the motion within the CR3BP and is a function of the Earth-Moon rotating position and velocity states. By evaluating the Jacobi Constant function from Equation (3) with states from the BCR4BP, the instantaneous Jacobi Constant value is obtained. The instantaneous Jacobi Constant value is not an integral of the motion in the BCR4BP due to the addition of the Sun. To illustrate the variation in the instantaneous Jacobi Constant value, consider the BLT computed in the BCR4BP and displayed in Figure 2(a). The transfer requires a duration of 100 days and departs from a 150 km altitude Low Earth Orbit (LEO) to be delivered into an L_2 Lyapunov orbit with a Jacobi Constant value of 3.124. The black circle represents the Moon's orbit. The instantaneous Jacobi Constant value along the BLT is evaluated in Figure 2(b), beginning at a value of 0.842 and ending at a value that precisely matches the Lyapunov orbit. The yellow squares are placed at 25-day intervals along both the transfer and Jacobi Constant curves. When the trajectory is closer to the Earth-Moon system, i.e., during the first and last 10 days of the transfer, the instantaneous Jacobi Constant value is near-constant. Conversely, the instantaneous Jacobi Constant value varies greatly when the transfer is further from the Earth and Moon and is more dominated by solar perturbations. The variation in the energy-like quantity is one metric for understanding the Sun's influence on pathways to the Moon.

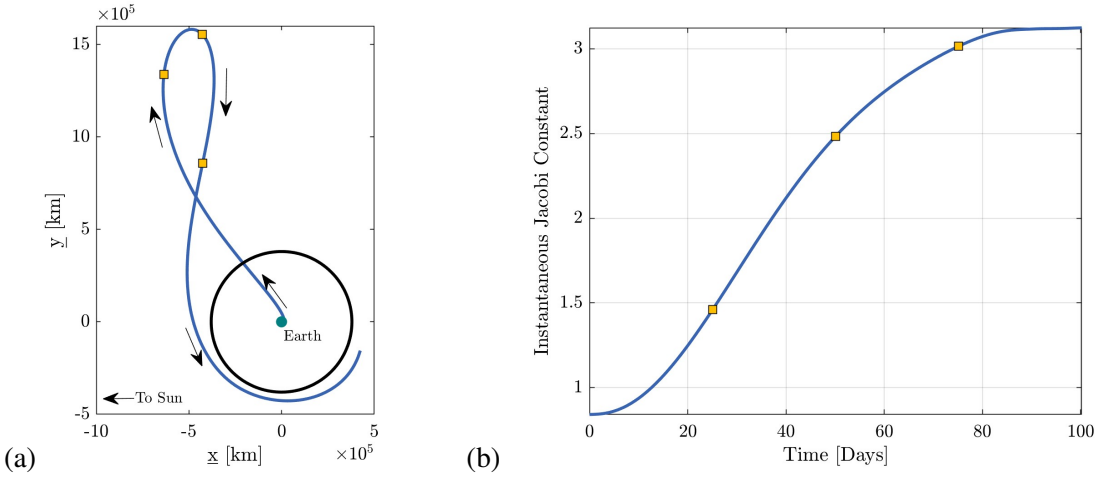

Figure 2. (a) Ballistic lunar transfer from a 150 km altitude LEO to an L_2 Lyapunov orbit, BCR4BP solution in the Sun-B_1 frame. (b) Evolution of the instantaneous Jacobi Constant value along the BLT

Low-thrust Augmented Four-body Problem

A dynamical model that incorporates the Earth, Moon, Sun, and low-thrust acceleration is employed to identify lunar transfers. The introduction of a low-thrust force increases the complexity and dimensionality of the solution space. Note that a transfer arc in the ballistic BCR4BP relies on eight variables, three position, three velocity, a Sun angle (epoch), and the propagation time. The introduction of low-thrust acceleration increases the dimensionality of the problem, as the control law can vary in direction and magnitude as a function of time. Therefore, the identification of available structures is dependent on the selected control laws. The thrust vector in the Earth-Moon rotating coordinate frame is labeled $\vec{\tilde{T}}$. The low-thrust acceleration vector is determined as $\tilde{a}_{LT} = \frac{\vec{\tilde{T}}}{m_3}$,

where the mass of the spacecraft is continually modified as,

$$\dot{m}_3 = -\frac{T}{\text{Isp}\, g_0} \tag{6}$$

The term Isp is the specific impulse for the low-thrust engine, and g_0 is the mean gravitational acceleration at Earth's surface (9.8067 m/sec^2). The acceleration of P_3 due to the BCR4BP low-thrust model is,

$$\ddot{\widetilde{x}}_{LT} = \ddot{\widetilde{x}} + \frac{\widetilde{T}_x}{m_3} \quad \text{(7a)} \qquad \ddot{\widetilde{y}}_{LT} = \ddot{\widetilde{y}} + \frac{\widetilde{T}_y}{m_3} \quad \text{(7b)} \qquad \ddot{\widetilde{z}}_{LT} = \ddot{\widetilde{z}} + \frac{\widetilde{T}_z}{m_3} \quad \text{(7c)}$$

where the variables $\ddot{\widetilde{x}}, \ddot{\widetilde{y}}$ and $\ddot{\widetilde{z}}$ represent the equations of motion for the ballistic BCR4BP. Cox assumes a constant mass low-thrust policy that aids in the identification of effective multi-body dynamical structures.[9] The constant mass policy is applied to this analysis to reduce the available low-thrust options. Assuming a constant thrust magnitude and mass, the low-thrust BCR4BP is defined by an acceleration vector. Dynamical systems theory provides insight into reducing the dimensionality of the problem. For low-energy transfers, a multi-body energy analysis enables the determination of desirable insertion conditions.[10] To produce low-thrust transfers that aid in energy reduction, the low-thrust acceleration vector is aligned with a rotating velocity direction.[9,11] As the equations of motion for the BCR4BP may be represented in either an Earth-Moon or Sun-B_1 rotating frame, both velocity directions become an option. For transfers to cislunar orbits, the aim is to increase the instantaneous Earth-Moon Jacobi Constant value prior to arrival in the Moon vicinity. Therefore, the low-thrust acceleration vector is constrained to be aligned with the Earth-Moon rotating velocity/anti-velocity direction. The velocity-aligned constant mass low-thrust policy in the BCR4BP is written as,

$$\ddot{\widetilde{x}}_{LT} = \ddot{\widetilde{x}} + \widetilde{a}_{LT}\frac{\widetilde{v}_x}{\widetilde{v}} \quad \text{(8a)} \qquad \ddot{\widetilde{y}}_{LT} = \ddot{\widetilde{y}} + \widetilde{a}_{LT}\frac{\widetilde{v}_y}{\widetilde{v}} \quad \text{(8b)} \qquad \ddot{\widetilde{z}}_{LT} = \ddot{\widetilde{z}} + \widetilde{a}_{LT}\frac{\widetilde{v}_z}{\widetilde{v}} \quad \text{(8c)}$$

where $\widetilde{v}$ is the scalar velocity in the Earth-Moon rotating frame, and $\widetilde{v}_i$ is the i^{th} component of the Earth-Moon rotating velocity vector. Given the assumptions in the control strategy, only one dimension is added to define a transfer arc in the low-thrust BCR4BP. The investigation aims to generalize the structures by introducing low-thrust capabilities to a spacecraft enroute to the Moon.

Substantiation of the fixed acceleration policy is key to support a valid low-thrust assumption. To explore the variation in mass along a thrusting arc, consider Equation (6). The following integral evaluates a change in mass along a thrusting arc,

$$\Delta m_3 = \int_{t_1}^{t_2} \dot{m}_3 dt$$
$$\Delta m_3 = -\int_{t_1}^{t_2} \frac{T}{\text{Isp}\, g_0} dt$$

where the integral is evaluated from the starting time t_1 to the final time t_2. For a thrusting arc, the initial mass is written as $m_{3,0}$. For any time beyond the initial time, the mass of the vehicle must be less than or equal to the starting mass. To produce some specified low-thrust acceleration value, the thrusting force must equal the product of the mass of the vehicle and the constant acceleration. As the mass is maximized at the initial time, the maximum force required to yield a given acceleration

level also occurs at the initial time. Thus, to generate an upper bound for the mass usage, the change in mass is rewritten as,

$$\Delta m_3 = -\int_{t_1}^{t_2} \frac{m_{3,0} a_{LT}}{\text{Isp}\, g_0} dt$$

Dividing both sides by the initial mass of the spacecraft ($m_{3,0}$) yields a mass fraction, i.e.,

$$\frac{\Delta m_3}{m_{3,0}} = \int_{t_1}^{t_2} \frac{a_{LT}}{\text{Isp}\, g_0} dt$$

Under the assumptions that the low-thrust acceleration and specific impulse are constant over time, the equation is reduced to,

$$\frac{\Delta m_3}{m_{3,0}} = \frac{a_{LT}(t_2 - t_2)}{\text{Isp}\, g_0} \tag{9}$$

For a given low-thrust acceleration and specific impulse values, Equation (9) delivers an estimate for the upper bound for mass fraction usage to complete a low-thrust arc. As an example, consider a sample vehicle matching the specifications for the Lunar Icecube mission, Isp = 2500 sec, F = 0.9 mN, the total mass of $m_{3,0}$ = 14 kg, and 1.5 kg of propellant.[5] As most BLTs require several months to reach the Moon, assume the low-thrust time-of-flight to be 90 days. Leveraging Equation (9), the mass fraction for a 90-day low-thrust arc is approximately 2%, well below 10% of propellant available. The constant acceleration policy is applied in this analysis to simplify the number of free variables when introducing low thrust and maintaining the underlying dynamical structures.

CHARACTERISTICS OF LOW-ENERGY TRANSFERS

Acknowledging each element of low-energy transfers aids in the construction of a mission-specific, desirable path. Time-of-flight and propellant costs are quickly identified as the two significant quantities associated with a BLT. However, a vehicle with a low-thrust engine may have excess propellant reserves but is not capable of implementing large maneuvers. Additionally, the propellant usage at launch or for the trans-lunar injection (TLI) is often evaluated differently than the propellant required for lunar orbit insertion, i.e., the propulsive capabilities of the launch vehicle rather than the spacecraft. Balancing such mission specifications is a nontrivial task in astrodynamics. However, a framework to address these challenges determines the viability of the transfer design.

Departure from the Earth-Moon system dominates the overall structure of any low-energy lunar transfer. Both ballistic and low-thrust paths rely on the relative orientation of the Earth-Moon-Sun system. Slight adjustments to the departure epoch, TLI magnitude, and/or departure direction introduce a major influence on the transfer geometries required to reach the lunar vicinity. Secondary payloads often face many challenges due to the lack of control over this initial departure phase. With control over the departure phase, proper use of lunar passes reduces the time-of-flight and TLI maneuver magnitude.

A lunar flyby may reduce both time-of-flight and propellant cost, thus, an overview of the departure conditions from Earth is required. For the sample transfers in this analysis, the parking orbit

about the Earth is assumed as a 150-km altitude, circular, LEO. The transfer from the Earth to the Moon lies in the same plane as the Earth, Moon, and Sun as modeled in the BCR4BP. As the TLI maneuver magnitude increases, there is also an increase in the energy of the spacecraft, i.e., a decrease in the instantaneous Jacobi Constant value evaluated at TLI. For purely ballistic transfers in the BCR4BP, the only source of modifying the instantaneous Jacobi Constant is through solar perturbations. Therefore, higher TLI magnitude requires the spacecraft to pass through regions where the force from the Sun's perturbations is higher in magnitude, or where the spacecraft is exposed to such perturbations over a longer time interval. These two conditions are typically not independent, as raising the apogee increases the perturbation magnitude and overall time-of-flight. However, the opposite also occurs. Reducing the TLI magnitude requires less of a requirement from solar perturbations to reduce the energy of the spacecraft prior to arrival at the Moon. In practice, there is a lower bound to this process. If the TLI is reduced too far, then the spacecraft remains in the Earth-Moon vicinity, and the solar forces are not sufficient to alter the geometry of the path. One way to reduce the TLI is through the use of a lunar flyby. Close passes to the Moon allow the spacecraft to pass through the L_2 portal at higher Jacobi Constant values. An example of a BLT that leverages an outbound lunar flyby is demonstrated in Figure 3(a). Similar to the transfer represented in Figure 2(a), the trajectory arrives into an L_2 Lyapunov orbit with a Jacobi Constant value of 3.124. The black circle indicates the orbit of the Moon, and the arrows mark the direction of travel. The altitude at the closest approach to the Moon for this transfer is 13177 km. The plot in Figure 3(b) is the progression of the instantaneous Jacobi Constant value along the BLT. The originating Jacobi Constant value equals 1.779. The yellow squares for both Figure 3(a) and Figure 3(b) mark the progression of time, where they are separated by 25 days along the transfer. Since this is the BCR4BP, there is no sudden jump in the Jacobi Constant value at the lunar flyby. Rather the gradual change exists due to solar forces. The overall time-of-flight for the transfer is 85.66 days, which is approximately two weeks shorter than the transfer from Figure 2(a). The TLI maneuver magnitude for the BLT in Figure 3(a) is 3.171 km/sec, approximately 45 m/sec lower than the example from Figure 3(a). A notable challenge associated with an outbound flyby is the dependency on the launch epoch, however; for the lunar pass to be viable, the post-flyby geometry must be directed toward a region that reduces the energy of the spacecraft prior to arrival into the desired orbit.[10,12]

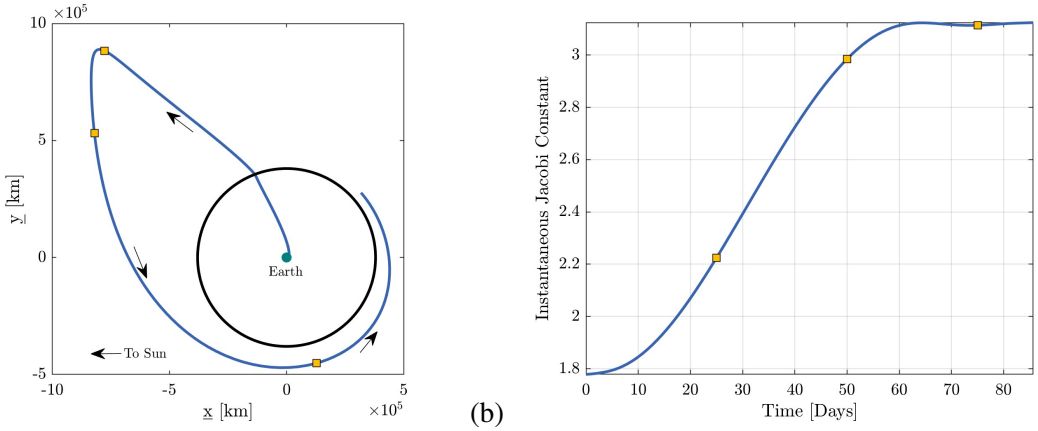

Figure 3. (a) Ballistic lunar transfer from a 150-km altitude LEO to an L_2 Lyapunov orbit, BCR4BP solution in the Sun-B_1 frame. (b) Evolution of the instantaneous Jacobi Constant value along the BLT

The cislunar destination guides the expected lunar orbit insertion (LOI) costs and may influence time-of-flight. Propellant cost is one of the driving factors in leveraging a BLT. Lunar orbit insertion may be constrained by spacecraft thrust limitations or propellant requirements. The insertion ΔV costs vary from near ballistic to several hundred meters per second depending on the intended destination. Unstable orbits offer minimal to no insertion costs by leveraging invariant manifold geometries. The transfer geometries in Figure 2(a) and Figure 3(a) both arrive ballistically into an L_2 Lyapunov orbit, with no insertion maneuver necessary to arrive into the unstable libration point orbit. Near-stable or stable orbits often require an LOI burn to insert into the desired structure. Previous investigations explore impulsive LOI maneuvers into a Near Rectilinear Halo Orbit (NRHO).[13] Scheuerle and Howell identify families of BLTs into a 9:2 NRHO with impulsive LOI maneuver ranging from 15 to 50 m/sec. Insertion into low lunar orbits (LLOs) often requires an LOI maneuver cost of several hundred meters per second. Previous investigations identify a strategy for approximating the theoretical minimum maneuver magnitude necessary to insert into a conic LLO along a BLT.[12] For example, the theoretical minimum LOI burn to circularize a BLT into a 100 km altitude LLO is 632 m/sec. Knowledge of approximate LOI maneuver costs aids in the design process for low-energy transfers.

Placement of Low-thrust Segments

The introduction of a low-thrust force offers a wide range of control authority over the desired path. In this investigation, the focus is on time-of-flight reduction through an energy analysis. The low-thrust policy assumes the thrust direction is always aligned opposite to the Earth-Moon rotating velocity vector. Such a strategy maximizes the growth in the Earth-Moon Jacobi Constant value. However, the rate of change of the Jacobi Constant value will also vary along a thrusting arc. The Jacobi Constant value for the CR3BP may be written as,

$$JC = 2U - \int \dot{\vec{r}} \cdot \ddot{\vec{r}} d\tau$$

where τ is nondimensional time. Note that for a low-thrust force applied in the CR3BP, the instantaneous Jacobi Constant value expression becomes,

$$JC_{ins} = 2U - \int \dot{\vec{r}} \cdot (\ddot{\vec{r}} + \vec{a}_{LT}) d\tau$$

The derivative of both sides with respect to nondimensional time renders the variation in the Jacobi Constant value,

$$\dot{JC}_{ins} = -\dot{\vec{r}} \cdot \ddot{\vec{r}} - \dot{\vec{r}} \cdot \vec{a}_{LT}$$

Note that the terms $\dot{\vec{r}} \cdot \ddot{\vec{r}}$ equates to zero when the acceleration vector is the nondimensional rotating acceleration derived from the CR3BP. Thus, the equation is simplified to the following expression,

$$\dot{JC}_{ins} = -\dot{\vec{r}} \cdot \vec{a}_{LT}$$

As the low-thrust policy employs acceleration directions opposite to the Earth-Moon velocity vector, the dot product yields,

$$\dot{JC}_{ins} = a_{LT} \dot{\vec{r}} \tag{10}$$

Equation (10) illustrates the variation in the Jacobi Constant value for a low-thrust strategy applied in the CR3BP, such that the low-thrust acceleration is constant and always directed opposite to the

rotating velocity vector. Note that the BCR4BP also incorporates solar perturbations in addition to the variations in the Jacobi Constant value. The insight from Equation (10) is derived from the same analysis as the Oberth effect.[9,11] Placing maneuvers where the spacecraft is moving at a higher Earth-Moon rotating speed leads to a larger change in energy. For cislunar transfers, such a strategy often leads to maneuvers placed near the Earth and Moon. However, when considering the instantaneous Jacobi Constant value, the relevant velocity is measured in the Earth-Moon rotating frame. A transfer that extends beyond the orbit of the Moon also possesses a relatively high speed. An example of the Earth-Moon velocity magnitude and its evolution along a BLT is illustrated in Figure 4 for the reference trajectory depicted in Figure 2(a). The yellow squares mark the same 25-day intervals along the 100-day transfer. As the transfer departs from the Earth near day zero, the Earth-Moon speed is at its maximum throughout the transfer. However, the high-velocity magnitude is brief as the magnitude decreases a few days into the transfer. Another extremum in the rotating velocity magnitude occurs at apogee, however, approximately 41 days along the path. Since the

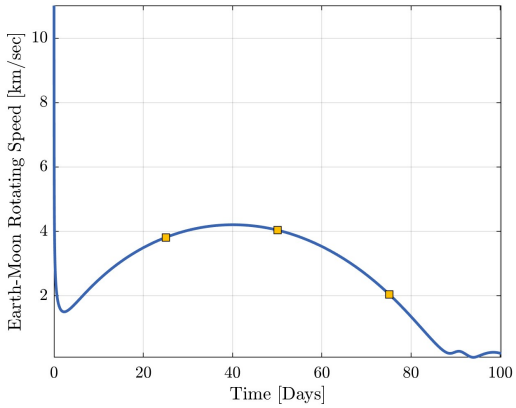

Figure 4. Evolution of the Earth-Moon rotating speed for the BLT from Figure 2(a)

aim is maximizing the change in the Jacobi Constant value, Equation (10) demonstrates that low thrust is ideally implemented over regions where the rotating velocity magnitude is greatest. With a constant low-thrust acceleration policy, the regions under the curve in Figure 4 are proportional to the change in the Jacobi Constant value. Consider a sample scenario where a 10-day thrusting arc is incorporated into the lunar transfer from Figure 2(a). To reduce the overall time-of-flight, and assuming only a single thrusting arc, the goal is to identify a desirable location to place the thrusting arc. Leveraging the insight from Equation (10) and the velocity evolution in Figure 4, from an energy analysis, the 10-day thrusting arc with the most influence is centered at apogee. Parrish et al. identify a similar strategy for placing a deterministic maneuver along a BLT for CAPSTONE operations.[1] To test the hypothesis, three transfers are generated with the ballistic solution from Figure 2(a) applied as the initial guess. The transfers are plotted in Figure 5. Transfers that incorporate the combined influence of low thrust and solar perturbations to reach the Moon are denoted as Cislunar Low-Energy Flight path (CLEF). The red segments are thrusting arcs, with a fixed low-thrust acceleration magnitude of 0.1 $\frac{mm}{s^2}$ and fixed 10-day thrusting arcs. The first CLEF in Figure 5(a) initiates the thrusting arc immediately after TLI and continues for the first 10 days of the flight. The second CLEF, illustrated in Figure 5(b), begins near apogee, approximately 35 days into the flight, and thrust is active until the 45-day mark. Note that the spacecraft spends more time out near apogee, such that the red curve appears shorter in Figure 5(b) than in the other

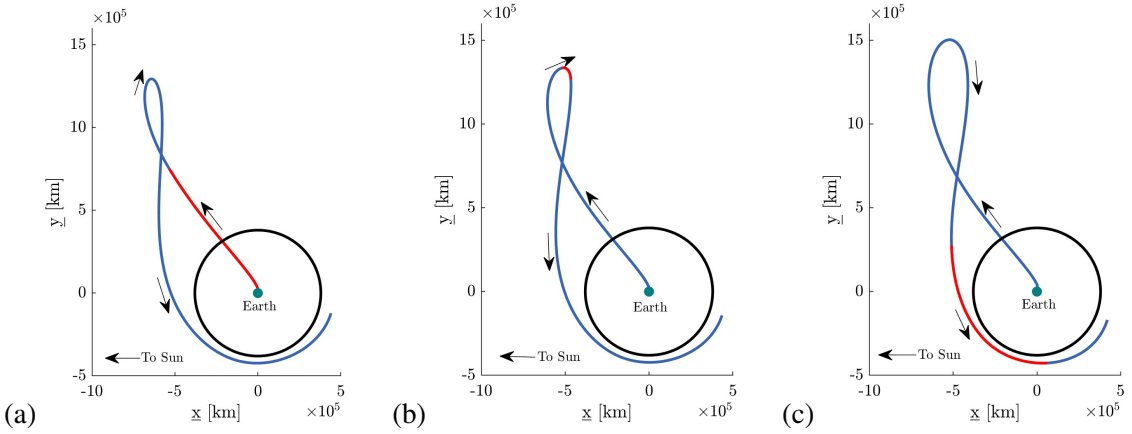

Figure 5. Low-energy transfers extended from Figure 2(a), 0.1 $\frac{mm}{s^2}$ low-thrust acceleration with the thrusting segment occurs from (a) day 0 to day 10 (b) day 35 to day 45, (c) day 80 to day 90

two examples. The third CLEF, in Figure 5(c), activates the thrust arc 80 days into the transfer. Recall that the baseline BLT includes a time-of-flight of 100 days. The time-of-flight for the CLEF transfers in Figure 5(a), Figure 5(b), and Figure 5(c) are 88.5, 85.6, and 95.8 days, respectively. For the 10-day thrusting examples, all three cases result in a reduction for time-of-flight. Following the hypothesis, applying the thrust segment near apogee yields the shortest total time-of-flight for the three scenarios, reducing the total transfer time by approximately two weeks. Observe that the first case, where the transfer time begins immediately after TLI (Figure 5(a)), is the second best option. And lastly, the third case, i.e., a thrusting arc when the spacecraft is near its slowest speed along the transfer (Figure 5(c)), reduces the time-of-flight by approximately 4.2 days. The time-of-flight reduction is associated with the change in the instantaneous Jacobi Constant value. To visualize the evolution of the energy-like quantity, Figure 6 illustrates the shift in the instantaneous Jacobi Constant value along the CLEF transfer from Figure 5(b). The blue and red curves represent ballistic and thrusting arcs, respectively. Note that the ballistic curves still posses a variation in the

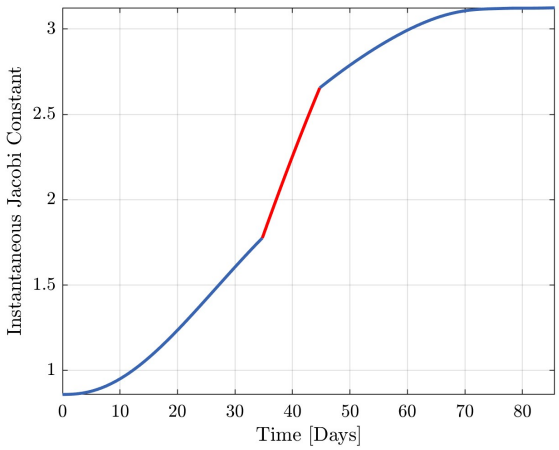

Figure 6. Evolution of the instantaneous Jacobi Constant value along the trajectory from Figure 5(b)

Jacobi Constant value due to solar perturbations. As the slope of the red curve is a function of the combined solar and low-thrust perturbations, an increase in the low-thrust acceleration would also increase the slope of the red curve.

Balancing of the various mission constraints is advantageous to recognizing possible transfer design strategies. The CLEF transfer from Figure 5(b) reduces the time-of-flight over roughly two weeks by simply employing a 10-day low-thrust strategy. Simultaneously, a purely ballistic solution is in Figure 3(a) that also reduces the time-of-flight by nearly the same amount, but alternatively leverages an outbound lunar flyby. The balance between these two techniques is a function of specific mission criteria. Some scenarios may require a wider launch period, such that an outbound flyby is not always available. Conversely, trajectory options may be limited by propellant requirements and chose to bypass a thrusting arc. The conditions are dependent on the specific mission requirements; the goal of this investigation is to offer insight and strategies to construct mission-desirable paths to the Moon.

CISLUNAR LOW-ENERGY FLIGHT PATHS

Low thrust is leveraged to generate transfer design options that could otherwise be infeasible with a purely ballistic solution. Several strategies are employed to identify possible transfer geometries. The first step in any process requires generating an initial guess. Three different techniques are applied in this analysis, labeled (i), (ii), and (iii). (i) The first strategy utilizes a predetermined BLT as the reference geometry. By replacing coasting arcs with pre-specified thrust arcs, a Newton-Raphson targeting algorithm is applied to maintain the desired mission constraints. This first strategy is employed for the example in Figure 5, where each initial guess originated from the converged BLT illustrated in Figure 2(a). The strategy of simply adding thrusting arcs to a BLT is advantageous if the goal is maintaining the preexisting geometry for the transfer. (ii) The second approach is similar to the first, as it requires a converged solution. However, the second strategy allows impulsive maneuvers along the baseline. Thrusting arcs are placed around the maneuvers with the aim to remove the maneuvers. (iii) The third methodology to deliver an initial guess leverages a low-thrust periapse Poincaré map. The periapse Poincaré map is generated by propagating states in reverse time from the desired orbit near the Moon and recording each perigee that occurs along a 100-day arc. However, the propagation also assumes a constant thrust arc applied throughout the entire transfer. The third strategy results in a more expensive initial guess while enabling dynamical structures that would otherwise go undetected in the ballistic cases.

Scenario A: Augmented Ballistic Lunar Transfers

To illustrate results from the three different initial guess strategies, a sample scenario is examined. Assume a spacecraft includes a low-thrust engine that achieves an acceleration level of 0.05 $\frac{mm}{s^2}$, with a specific impulse of 2500 s. Again, the goal is to depart from a 150-km altitude LEO and flow into a L_2 Lyapunov orbit in the Earth-Moon system. (i) A ballistic transfer solution is applied to construct the first initial guess. Thrusting arcs are added near apogee consistent with the insight gained from Figure 5. A natural parameter continuation scheme is employed to decrease the overall time-of-flight of the transfer. Three members of the family are included in Figure 7. All three transfers include thrust arcs with the force in the opposite direction of the Earth-Moon rotating velocity. The constant low-thrust acceleration along the thrust arcs is 0.05 $\frac{mm}{s^2}$, i.e., the same level as the sample scenario. Each transfer is depicted in the Sun-B_1 rotating reference frame and is constructed in the low-thrust BCR4BP. The blue segments of the transfer indicate ballistic arcs,

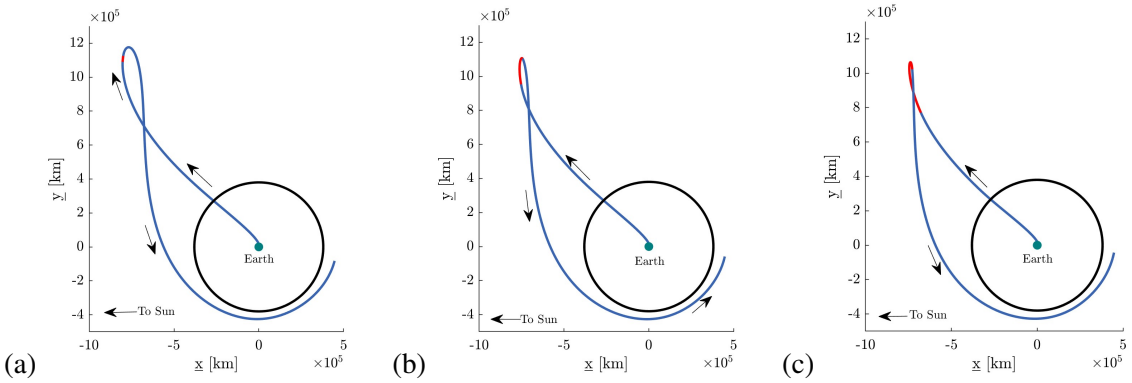

Figure 7. Low-energy transfers with varying thrust duration, 0.05 $\frac{mm}{s^2}$ low-thrust acceleration (a) 2.5 days, (b) 15 days, (c) 25 days

while the red sections denote a thrust arc. The CLEF transfer in Figure 7(a) includes a thrusting arc with a duration of 2.5 days, and an 87.8-day time-of-flight. The trajectory illustrated in Figure 7(b) has a 15-day thrust arc and an 83.2-day time-of-flight. The path in Figure 7(c) illustrates a 25-day thrust arc and a flight duration of 80.4 days. (ii) The second initial guess strategy employs a transfer strategy with impulsive maneuvers placed along the trajectory and then removed. To align with the previous results, a maneuver is placed near apogee to aid in modifying the instantaneous Jacobi Constant value. The initial guess employed for the second strategy appears in Figure 8. The impulsive maneuver is indicated by the red dot and includes a magnitude of 150 m/sec. The time-of-flight for the initial guess is 84.8 days, with a 7800 km altitude outbound lunar flyby. To replace the impulsive maneuver, an estimate for the duration of the thrust arc is necessary. A simple estimate divides the total maneuver magnitude by the acceleration level of the vehicle. For the 150 m/sec maneuver and a low-thrust acceleration of 0.05 $\frac{mm}{s^2}$, the estimate for the thrust duration is 34.8 days. Given the new initial guess, a family of transfers is constructed via a continuation process in decreasing time-of-flight. Three members of the family appear in Figure 9. The black circle in each plot represents the orbit of the Moon in the BCR4BP. The CLEF transfer illustrated in Figure 9(a) is the first converged solution from the initial guess. The solution is constrained to retain the same

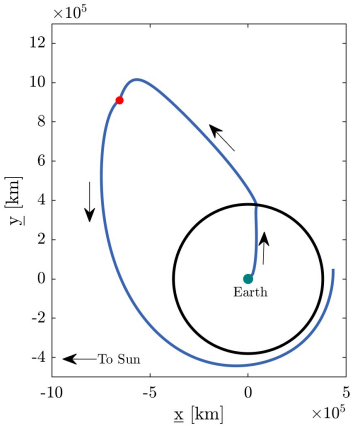

Figure 8. Low-energy trajectory employed as the initial guess for the CLEF transfer design, the red dot indicates the location of a 150 m/sec impulsive maneuver

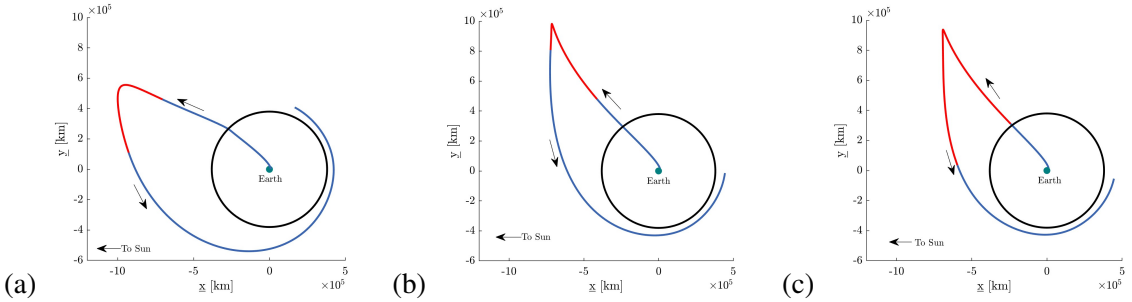

Figure 9. Low-energy transfers constructed from an impulsive maneuver initial guess, 0.05 $\frac{mm}{s^2}$ low-thrust acceleration, and total flight duration of (a) 84.8 days, (b) 75.3 days, (c) 69.8 days

time-of-flight as the initial guess (84.8 days), with a thrust duration of 38.2 days, slightly longer than the estimate. The arc from Figure 9(b) is delivered by a time-of-flight of 75.3 days with a 36.2 day thrust arc. The trajectory plotted in Figure 9(c) also from the family of transfers completes the path with a flight duration of 69.8 days and a thrust arc of 52.1 days. (iii) The third initial guess strategy leverages the low-thrust periapse Poincaré map. The map is constructed by propagating 10,000 points along the destination orbit (L_2 Lyapunov) in reverse time. The destination orbit is a periodic solution from the CR3BP. To accommodate for the epoch dependency in the BCR4BP, the process is repeated 10 times, with equally spaced intervals between the Sun angles of 0 and 2π. Each propagation assumes a constant low-thrust acceleration value of 0.05 $\frac{mm}{s^2}$. The periapse Poincaré map is illustrated in Figure 10. Each point denotes a separate perigee that is delivered to the L_2 Lyapunov orbit, plotted in the Earth-Moon rotating frame. The color of each point indicates the time-of-flight along the arc, where the increasingly cyan color corresponds to a shorter transfer duration. The green-filled circle represents the Earth, and the black circle is the 150 km altitude LEO. The plot is focused close to the Earth to represent transfers that may depart from LEO. Thus, the initial guess selected from the periapse Poincaré map is indicated by the red circle in Figure 10. The initial guess for the transfer is defined by a time-of-flight equal to 57 days and is represented in Figure 11(a). The transfer includes an outbound lunar flyby with an altitude of 6,500 km. Through natural parameter continuation in total transfer time yields a family of transfers, the flight duration

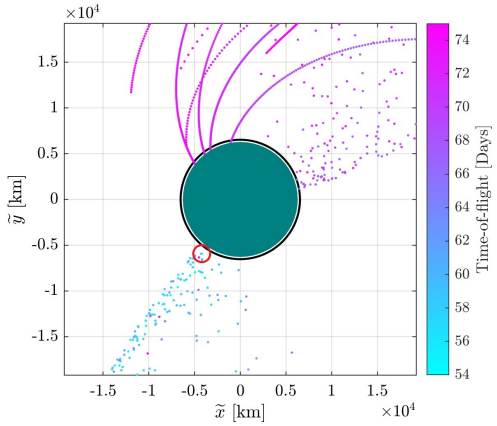

Figure 10. Periapse Poincaré map depicted in the Earth-Moon rotating frame, centered at the Earth

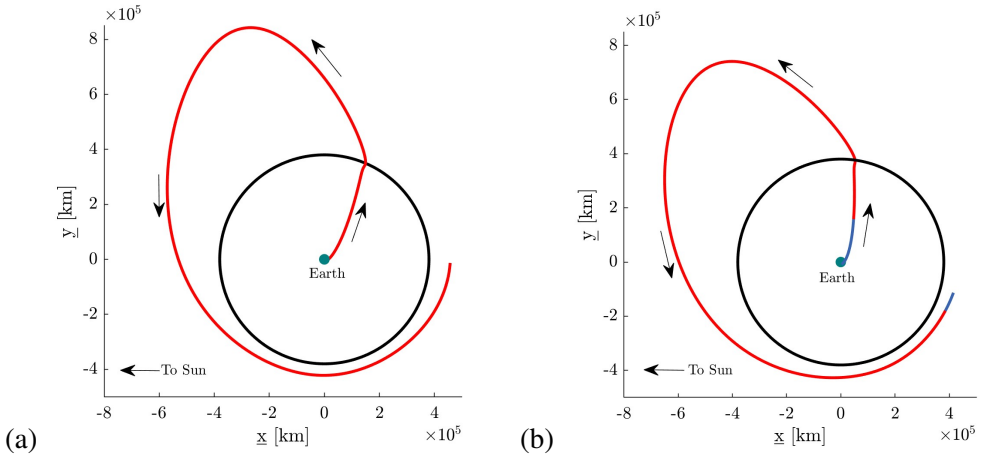

Figure 11. Low-energy transfers constructed from a periapse Poincaré map, with a 0.05 $\frac{mm}{s^2}$ low-thrust acceleration, and total flight duration of (a) 57 and (b) 54 days

for the shortest CLEF transfer is 54 days, illustrated in Figure 11(b). The trajectory in Figure 11(b) also leverages an outbound lunar flyby, with an altitude of 7600 km. The thrust arc is approximately 52.5 days. As evident in Figure 11, such short duration requires nearly continuously active low-thrust engines.

Mass Usage for Scenario A

Evaluating the propellant required to produce the time reductions in Figure 11, offers insight into the efficacy of the identified solutions. The three initial guess strategies offer a range of solutions, ranging from near-ballistic to entirely dependent on low thrust. To identify the required mass usage, the approximation from Equation (9) is applied. The thrusting arcs are converted to an estimate for the mass fraction required to complete such operations. The specific impulse assumed for this analysis is 2500 s, and any variation to this number is inversely proportional to the resultant mass fraction. The variation in mass fraction and time-of-flight is depicted in Figure 12. The three curves correspond to the families constructed through the different initial guess strategies. The arcs associated with Family 1 and Family 2 include nearly horizontal sections. These horizontal sections are correlated with the apogee of the trajectory shifting toward a region where solar perturbations are more dominant.[12,14] Family 1 and Family 2 also include a section that demonstrates the trade-off between time-of-flight and the required propellant mass. For example, the purple curve representing Family 1 depicts that reducing the total time-of-flight from 87 days to 80 days would cost additional propellant equivalent to roughly 0.45% of the mass of the vehicle. The gap that occurs between the families is due to the location of the Moon upon departure from Earth. The CLEF transfers to the L_2 Lyapunov orbit are planar, thus, interference with the Moon poses difficulty in the natural parameter continuation process. Additional insight is gained from Family 3. Similar to the example from the ballistic case in Figure 3(a), leveraging an outbound lunar flyby may aid in reducing the overall transfer time. The CLEF transfers from Family 3 incorporate thrusting arcs for nearly the entire path, while also employing an outbound lunar flyby. The combined effect yields the shortest time-of-flight solutions for this scenario. Comparing Family 3 to Family 2 further indicates the importance of such a flyby, as a slight increase in propellant yields a transfer solution that is two weeks shorter. Each strategy offers advantages and disadvantages in the mission design process, and

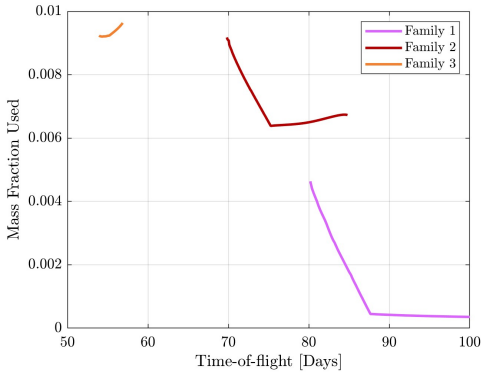

Figure 12. Evolution across time-of-flight and mass fraction for the transfer families generated in Figure 7 (Family 1), Figure 9 (Family 2), and Figure 11 (Family 3)

likely requires a balance between reducing the time along a trajectory and the propellant required to follow some desired geometry.

Scenario B: Transfers to a 9:2 NRHO

Low-thrust structures offer pathways to a three-dimensional 9:2 NRHO. Near rectilinear halo orbits offer several advantages as a destination orbit about the Moon, one key advantage being the low stationkeeping costs to maintain the orbit. The 9:2 NRHO is selected as a sample destination as this specific NRHO is the intended orbit for NASA's Gateway facility. The previous examples leverage the instability of the L_2 Lyapunov orbit. The unstable behavior allows transfers to follow the natural flow along the stable manifold structure into the desired orbit. However, insertion into the nearly stable 9:2 NRHO requires a maneuver. By employing the initial guess strategies previously detailed, the method that best suits this problem is the Poincaré map strategy. Rather than approximating each arc entirely as a thrusting arc, the segments are decomposed into a 120-day coast segment, followed by a 14-day thrust segment. For this example, a low-thrust acceleration level of 0.1 $\frac{mm}{s^2}$ is assumed. The initial guess selected from the periapse Poincaré map is illustrated in Figure 13(a), with a time-of-flight of 98 days, including the 14-day thrust segment necessary to insert into the NRHO. Through a natural parameter continuation procedure and continuation parameters defined as decreasing time-of-flight, a family of CLEF transfers is constructed and plotted in Figure 13. To leverage the insight gained from the earlier analysis, an additional thrust segment is placed near apogee to assist in reducing the overall time-of-flight. The overall time for the CLEF transfer in Figure 13(b) is 85.7 days, where the thrusting arcs are split between a 14.2-day segment near apogee and a 14.3-day segment prior to NRHO insertion. The trajectory illustrated in Figure 13(c) requires a 74-day time-of-flight, where the thrust arc near apogee is 50 days long and the thrust arc prior to NRHO insertion is 13 days long. Similar to the examples for transfers to a planar Lyapunov orbit, a trajectory that leverages an outbound lunar flyby and constant thrust is most straightforwardly identified by employing the periapse Poincaré mapping strategy. The low-thrust transfer to the 9:2 NRHO that leverages an outbound lunar flyby is depicted in Figure 14. The transfer evolves over 53.6 days to reach the NRHO, where a vast majority (53.1 days) require active thrust. The altitude of the outbound lunar flyby is 2500 km. The planar projection is plotted in Figure 14(a), and the out-of-plane component is illustrated by Figure 14(b).

A comparison of time savings against propellant usage for the NRHO CLEF transfers offers in-

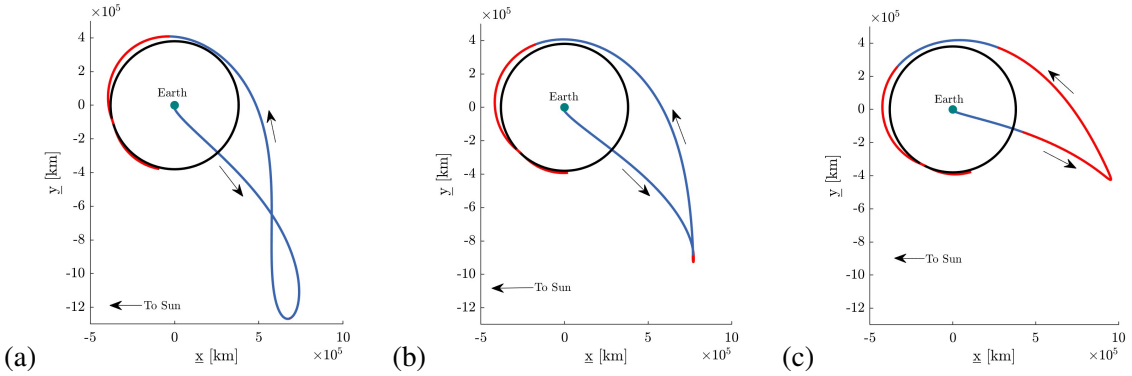

Figure 13. Low-energy transfers constructed from a periapse Poincaré map arriving into a 9:2 NRHO, with a 0.1 $\frac{mm}{s^2}$ low-thrust acceleration, and total flight duration of (a) 98 days, (b) 85.7 days, and (c) 74 days

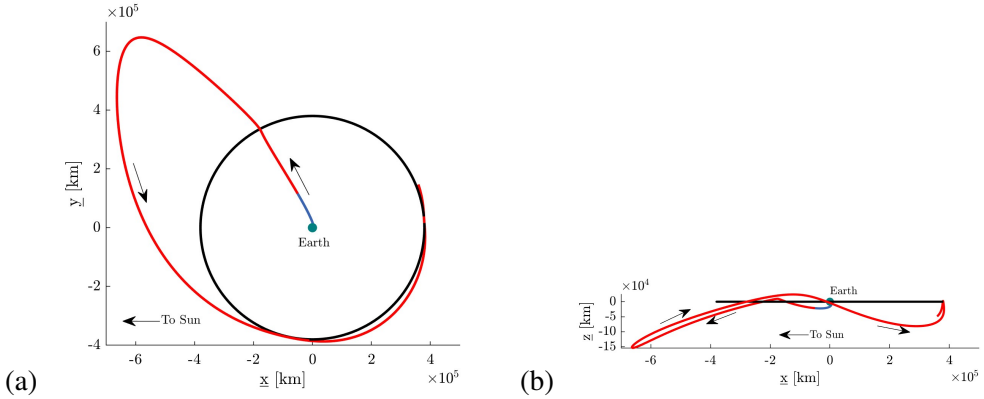

Figure 14. Low-thrust transfer to a 9:2 NRHO, 53.6-day flight duration and a low-thrust acceleration of 0.1 $\frac{mm}{s^2}$, plotted in (a) $\widetilde{x}\widetilde{y}$-plane and (b) the $\widetilde{x}\widetilde{z}$-plane

sight into the mission design process. Consistent with the previous procedure, the specifications for the scenario (low-thrust acceleration of 0.1 $\frac{mm}{s^2}$ and a specific impulse set to 2500 s) and evaluation of Equation (9) provides an approximation for the propellant necessary to complete the constructed paths. The tradeoff between the transfer duration and mass fraction is included in Figure 15. The purple curve represents the family from Figure 13, while the orange curve depicts the family constructed from Figure 14. Note that there are no purely ballistic solutions that arrive into the 9:2 NRHO, i.e., no solution exists near zero. Although the NRHO is nearly linear stable, some manifolds can be constructed but the energy gap must be bridged. For this sample scenario, roughly 0.5% of the mass of the spacecraft is necessary to insert into the NRHO. Another observation from Figure 15 is the efficiency of the flyby family in orange. As apparent in the previous example, incorporating an outbound lunar flyby may yield a shorter flight.

Low Thrust versus Solar Perturbations

Exploring low thrust options adds insight into the accessible regions throughout the Earth-Moon-Sun system. Although a low-thrust force aids the process of reaching the lunar vicinity, many of the transfers also rely heavily on solar perturbations to bridge the energy gap. The Sun is advantageous

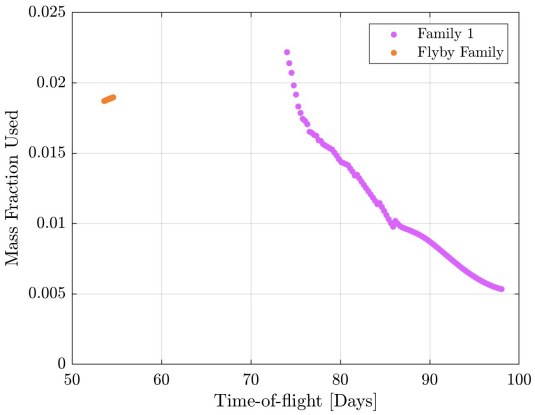

Figure 15. Trade-off between propellant required as a mass fraction and the flight duration across the CLEF transfers inserting into the 9:2 NRHO

to the trajectory given a specific relative orientation between the Earth and the Sun, i.e., the proper quadrant. Quadrants in the Sun-B_1 BCR4BP refer to four distinct regions and are often identified in terms of a Sun-B_1 view from Figure 1(b), labeled I, II, III, and IV as denoted in Figure 16(a). Scheuerle et al. explore the influence of quadrants on the Hamiltonian for a path.[10] The transfer from Figure 2(a) is a sample of a path that passes through quadrant II, whereas the transfers from Figure 13 travel through quadrant IV. For low-energy transfers to the Moon, the four quadrants are separated by the $\underline{x}$-axis and $\underline{y}$-axis in the Sun-B_1 rotating frame, centered about the Earth-Moon barycenter, B_1. When the spacecraft is in quadrants II or IV, the Sun's gravity aids in increasing the instantaneous Jacobi Constant value. In contrast, as the spacecraft moves through quadrants I or III, the solar perturbations increase the energy-like quantity, i.e., decreasing the instantaneous Jacobi Constant value. To explore the costs associated with working against solar perturbations, a new scenario is devised. Consider a vehicle that is capable of 0.2 $\frac{mm}{s^2}$ for a low-thrust acceleration, with a specific impulse of 2500s. The goal is again to arrive into an L_2 Lyapunov orbit. Leveraging the periapse Poincaré mapping technique for the initial guess, the transfer illustrated in Figure 16 is generated. The trajectory in Figure 16 requires a time-of-flight of 46.9 days, with a thrust segment that is 28 days long. The outbound leg includes a lunar flyby with an altitude of 15000 km above the surface. The curve in Figure 16(b) displays the same transfer in the Earth-Moon rotating frame. The apogee radius relative to Earth is 720,000 km and is located in quadrant II. Natural parameter continuation in Sun angle is applied to assess the influence of the solar perturbations. The time-of-flight is constrained to remain constant at 46.9 days. Members of the resulting family of CLEFs are plotted in Figure 17. The path in Figure 17(a) traverses mostly through quadrant I, resulting in a thrust arc that is continuous along the entire transfer; essentially, the low-thrust force must offset the solar perturbing force. The transfer depicted in Figure 17(b) traverses through quadrant III and also requires a thrusting arc along the entire transfer. In contrast, the transfer in Figure 17(c) passes through quadrant IV and leverages the solar force, with a thrust arc of only 28.9 days. Relative to the Earth-Moon system, the four solutions from Figure 16(a) and Figure 17 all possess similar geometry. The influence of solar perturbations differs, however, and the solar force acting with or against the desired geometry.

A relationship between the solar gravity perturbation, captured via apogee location and the resulting mass usage is further explored. Paths denoted in Figure 17 are a subset of the larger family of solutions. An apogee angle is introduced to evaluate the quadrant for the transfer. A schematic

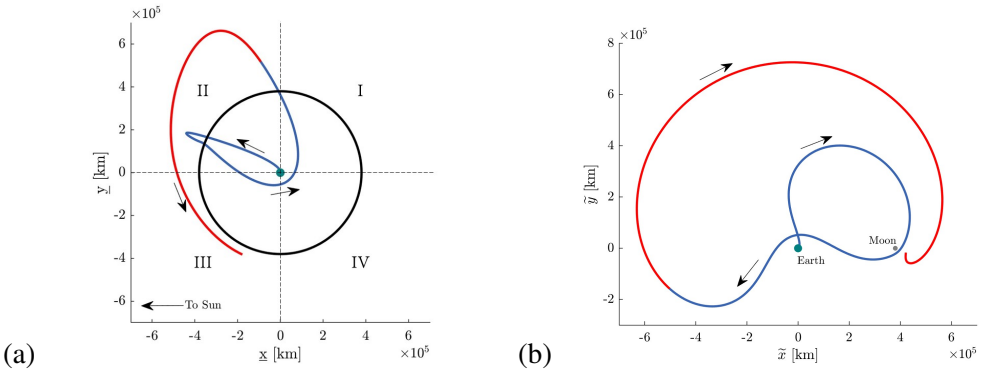

Figure 16. Low-thrust trajectory to an L_2 Lyapunov in the BCR4BP, represented in (a) the Sun-B_1 rotating frame and (b) the Earth-Moon rotating frame

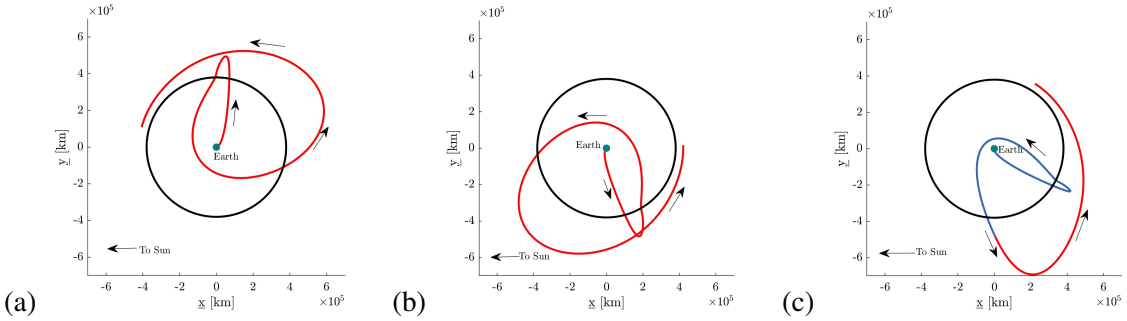

Figure 17. Low-energy transfers constructed from a periapse Poincaré map arriving into a L_2 Lyapunov, with a 0.2 $\frac{mm}{s^2}$ low-thrust acceleration and the apogee placed in (a) quadrant I, (b) quadrant III, and (c) quadrant IV

in Figure 18 demonstrates the definition of the apogee angle. The apogee angle (β) is measured from the $+\underline{x}$-axis to the vector connecting the Earth-Moon barycenter (B_1) to the furthest apogee, marked in black. The apogee angle for the transfer in Figure 18 is 32 degrees. The apogee angle is computed for each member of the constant time-of-flight family from which the transfers in Figure 17 are samples. The mass usage is estimated from Equation (9) assuming a specific impulse of

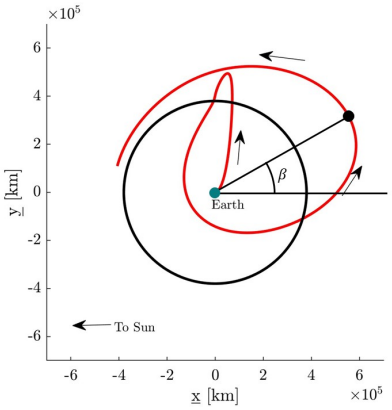

Figure 18. Schematic demonstrating the apogee angle along the transfer depicted in Figure 17(a)

2500s. The variation in mass usage across the apogee angle is illustrated in Figure 19. The mass fraction required reflects the propellant required as a function of the total mass of the spacecraft. The plot is clearly separated into four distinct quadrants, where quadrants I and III are colored red, while quadrants II and IV are noted in green. The variation in mass fraction demonstrates the effect of solar perturbations on the geometry. Note that this particular geometry possesses a relatively low apogee radius compared to other low-energy transfers. As the apogee distance increases, the Sun's effect on the geometry does grow.

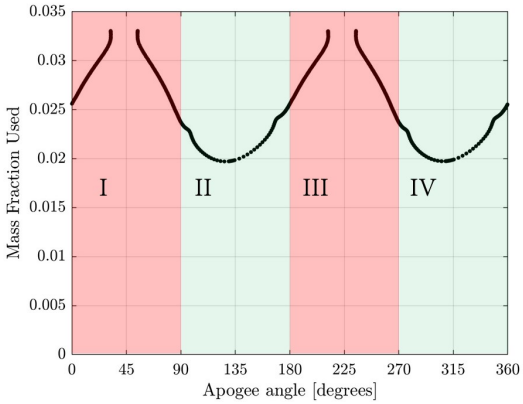

Figure 19. Evolution of mass usage with respect to the apogee angle for the fixed time-of-flight family of CLEF transfers, each with a time-of-flight of 46.9 days

CONCLUDING REMARKS

The goal of this preliminary investigation is a framework for generating transfers that leverage low-thrust and solar perturbations in the Earth-Moon-Sun system. The paper explores a set of assumptions that helps simplify the complexity of introducing low thrust into the transfer design process. By focusing on the primary goal of reducing time-of-flight, a simplified low-thrust strategy is applied. The assumptions are examined for a range of low-energy lunar transfer options. Through the application of a low-thrust design strategy, several options emerge for identifying initial guesses. Each approach offers advantages and disadvantages, directly related to the trade-off between propellant usage and overall time-of-flight. This effort explores energy variations due to the combined influence of solar gravity and low-thrust accelerations as a metric to evaluate performance. Leveraging low thrust and solar gravity simultaneously adds control over the time-of-flight, and overall transfer options when reaching the Moon. Transfer options include the ability to arrive into near-stable 3D orbits, i.e., 9:2 NRHO. Low thrust forces and solar perturbations influence a trajectory through different regions of space and insights into the trade-offs is key to the mission design process. With increasing low-thrust acceleration levels, the spacecraft can move through more quadrants in the Sun-B_1 rotating frame as necessary to satisfy mission constraints to access the lunar region. The passage through new regions of space is achievable as the acceleration imparted by low-thrust propulsion must overcome undesirable solar perturbations. Employing a low-thrust policy combined with solar perturbations offers an effective strategy for designing paths to cislunar space.

ACKNOWLEDGEMENTS

The authors would like to thank the School of Aeronautics and Astronautics at Purdue University, and the Rune and Barbara Eliasen Visualization Laboratory for facilities and financial support. Portions of this work are supported by NASA Johnson Space Center under Grant No. 80NSSC19K1175. The authors would also like to thank Brian McCarthy, Emily Zimovan-Spreen, and fellow members of the Purdue Multi-Body Dynamics Research Group for informative discussions.

REFERENCES

[1] N. L. Parrish, E. Kayser, S. Udupa, J. S. Parker, B. W. Cheetham, and D. C. Davis, "Ballistic Lunar Transfers to Near Rectilinear Halo Orbit: Operational Considerations," *AIAA Scitech 2020 Forum*.

[2] Y.-J. Song, Y.-R. Kim, J. Bae, J.-i. Park, S. Hong, D. Lee, and D.-K. Kim, "Overview of the Flight Dynamics Subsystem for Korea Pathfinder Lunar Orbiter Mission," *Aerospace*, Vol. 8, No. 8, 2021, 10.3390/aerospace8080222.

[3] J. Stewart, C. Hobbs, and S. Collins, "A Mission to the Moon," `https://coe.gatech.edu/news/2022/11/mission-moon-lunar-flashlight`, 2022.

[4] ispace, "HAKUTO-R Mission 1," `https://ispace-inc.com/m1`, 2022.

[5] N. Bosanac, A. D. Cox, K. C. Howell, and D. C. Folta, "Trajectory design for a cislunar CubeSat leveraging dynamical systems techniques: The Lunar IceCube mission," *Acta Astronautica*, Vol. 144, 2018, pp. 283–296, https://doi.org/10.1016/j.actaastro.2017.12.025.

[6] A. Hoffman, B. Park, T. Roorda, S. Stewart, and K. C. Howell, "Trajectory Design for a Secondary Payload within a Complex Gravitational Environment: The Khon-1 Spacecraft," *AIAA/AAS Astrodynamics Specialist Conference*, Charlotte, North Carolina, August 2022.

[7] V. G. Szebehely, *Theory of Orbits: The Restricted Problem of Three Bodies*. New York: Academic Press, 1967.

[8] A. E. Roy, *Orbital Motion*. Bristol: A. Hilger, 2nd ed. ed., 1982.

[9] A. D. Cox, "A Dynamical Systems Perspective for Preliminary Low-thrust Trajectory Design in Multi-body Regimes," *Ph.D. Dissertation*, West Lafayette, Indiana, May 2020, https://doi.org/10.25394/PGS.12206219.

[10] S. T. Scheuerle, B. P. McCarthy, and K. C. Howell, "Construction of Ballistic Lunar Transfers Leveraging Dynamical Systems Techniques," *AIAA/AAS Astrodynamics Specialist Conference*, 2020.

[11] H. Oberth, "Ways to Spaceflight," *NASA Technical Translation F-622*, Washington, DC, 1972.

[12] S. T. Scheuerle, "Construction of Ballistic Lunar Transfers in the Earth-Moon-Sun System," 2021. M.S. Thesis, Purdue University, West Lafayette, Indiana.

[13] S. T. Scheuerle and K. C. Howell, "Characteristics and Analysis of Families of Low-energy Ballistic Lunar Transfers," *AIAA/AAS Astrodynamics Specialist Conference*, August 2021.

[14] D. C. Davis and K. C. Howell, "Characterization of Trajectories Near the Smaller Primary in the Restricted Problem for Applications," *Journal of Guidance, Control, and Dynamics*, Vol. 35, No. 1, 2012, pp. 116–128.